Supporting Information

Facile synthesis of 3D N-doped porous carbon nanosheets as highly active electrocatalyst toward the reduction of hydrogen peroxide

Nannan Lu[a], Tingting Zhang[a], Xiaoyi Yan[a], Yue Gu[a], He Liu[a], Zhiqian Xu[a], Haixin Xu[a], Xuwen Li[a], Zhiquan Zhang*[a], Ming Yang*[b]

[a] Laboratory of Analytical Chemistry, College of Chemistry, Jilin University, Changchun 130012, China, E-mail: zzq@jlu.edu.cn

[b] Department of Breast Surgery, First Hospital, Jilin University, Changchun 130012, PR China. Email: yangming1967@163.com

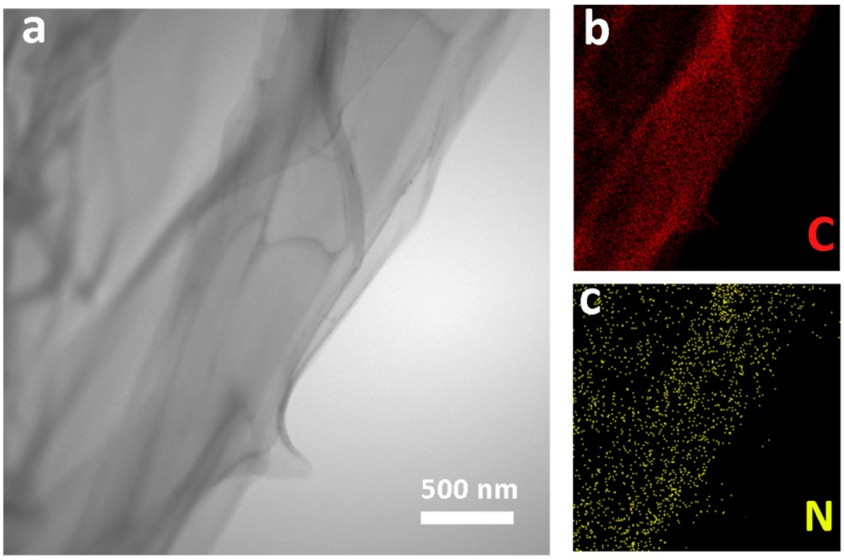

Fig. S1 (a) TEM image of 3D-NS-900 and corrosponding (b) C and (c) N elemental mapping.

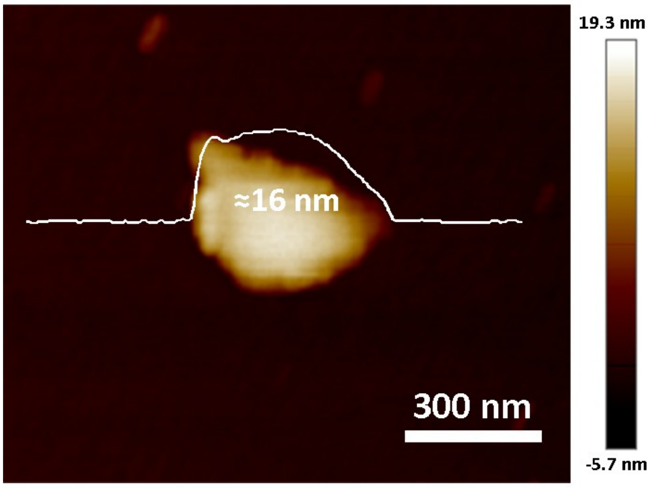

Fig. S2 AFM image of 3D-NS-900.

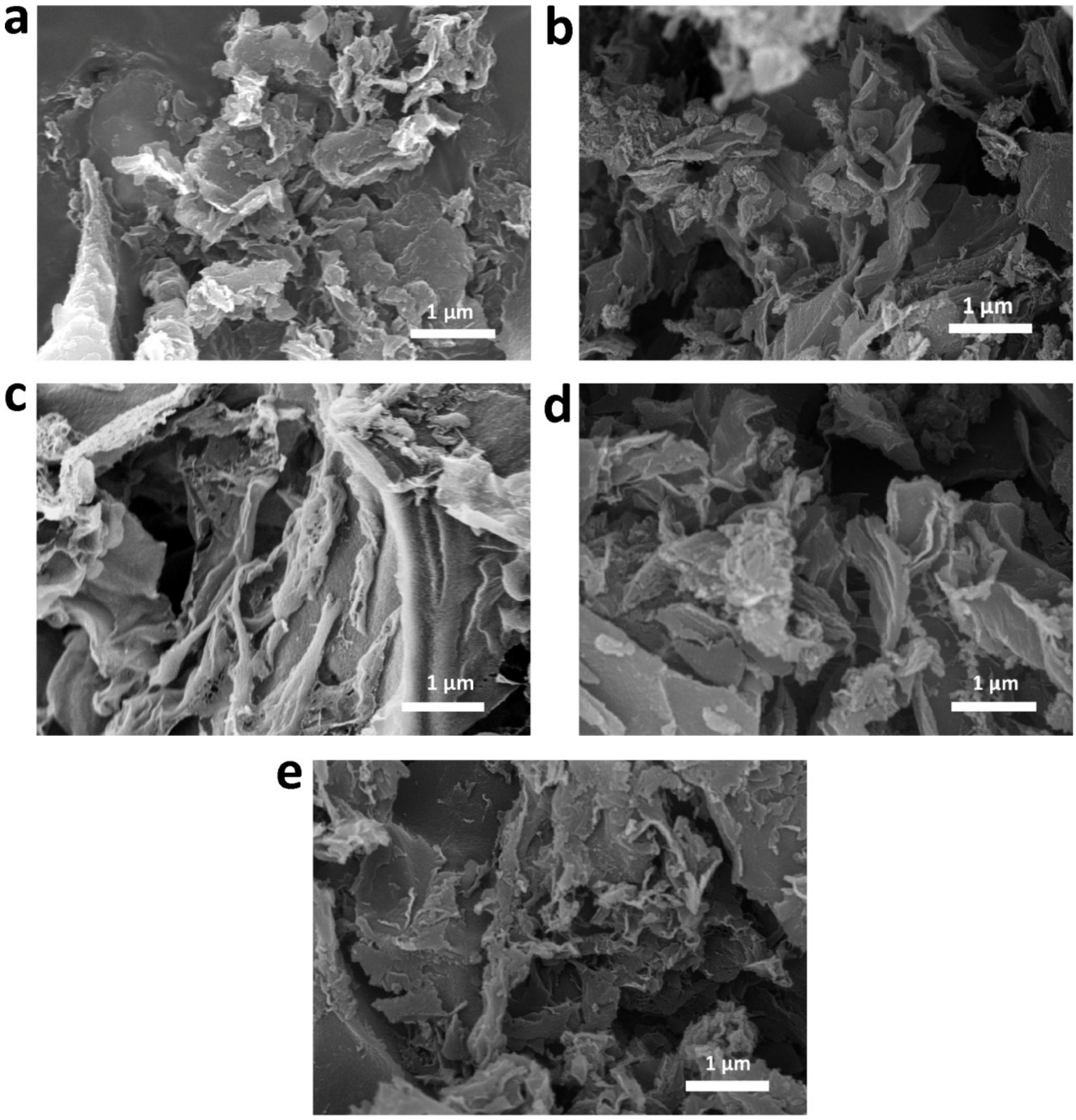

Fig. S3 FESEM images of (a) G-900, (b) 3D-NS-800, (c) 3D-NS-850, (d) 3D-NS-900 and (e) 3D-NS-950.

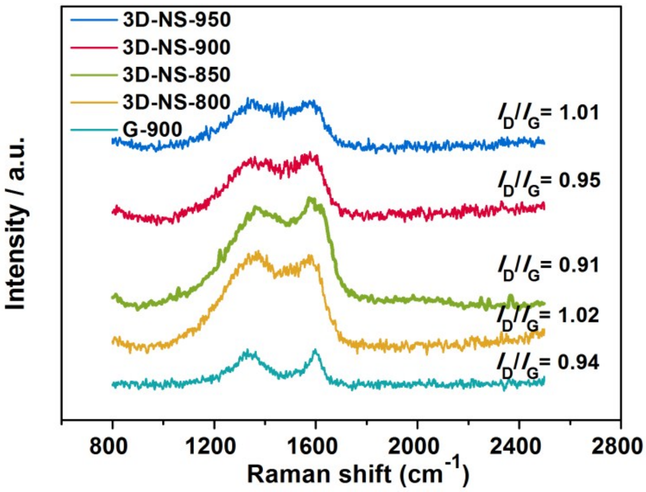

Fig. S4 Raman spectrum of G-900 and 3D-NSs.

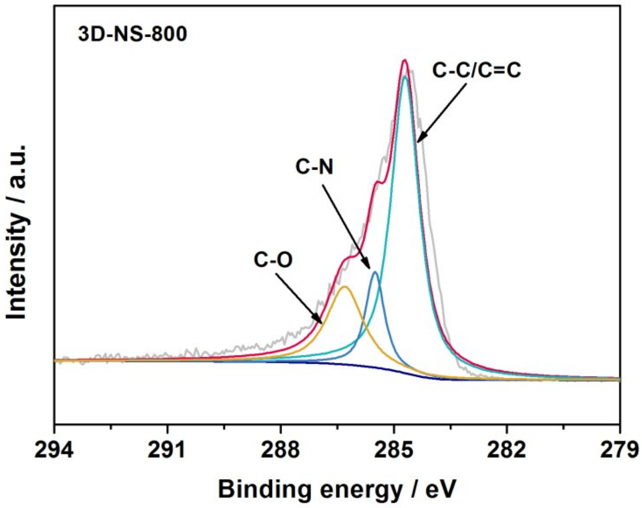

Fig. S5 The high-resolution spectra of C 1s of 3D-NS-800.

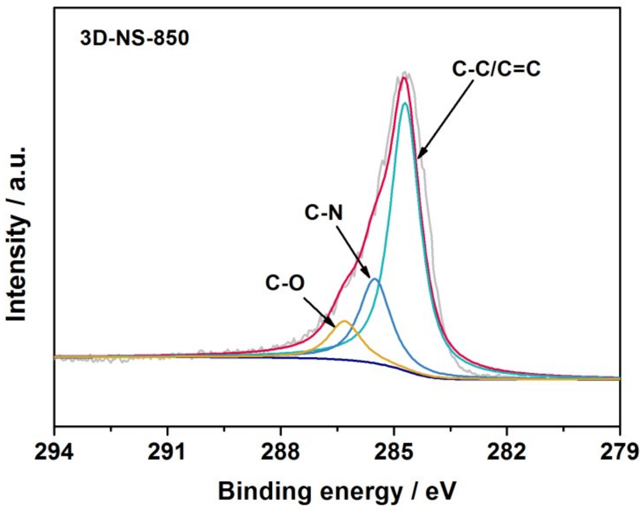

Fig. S6 The high-resolution spectra of C 1s of 3D-NS-850.

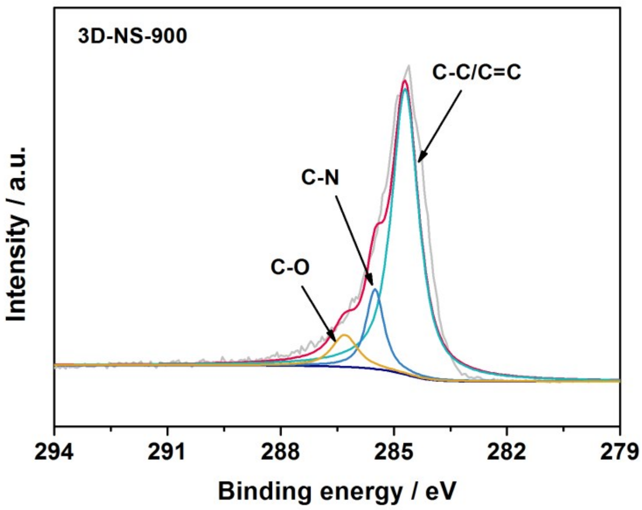

Fig. S7 The high-resolution spectra of C 1s of 3D-NS-900.

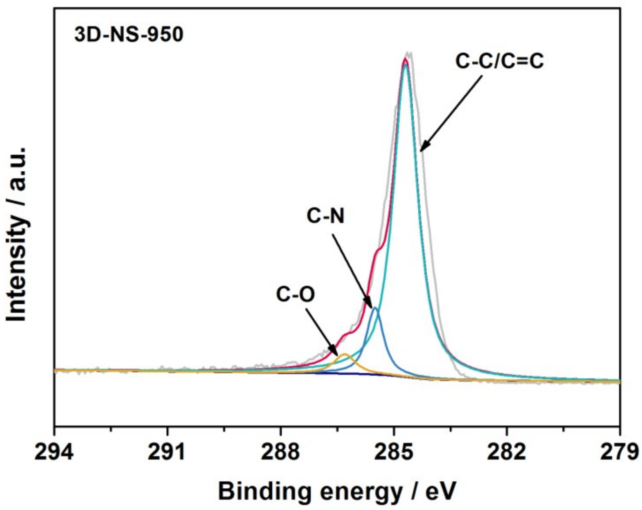

Fig. S8 The high-resolution spectra of C 1s of 3D-NS-950.

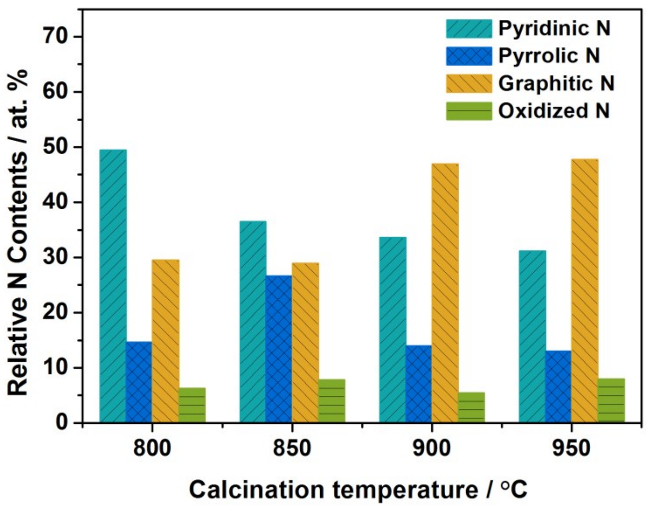

Fig. S9 The relative content of each N species of 3D-NSs.

Table S1 Results of element content of G-900 and 3D-NSs detected by XPS.

Samples	C (at. %)	N (at. %)	O (at. %)
G-900	91.43	– –	8.57
3D-NS-800	80.64	15.41	3.95
3D-NS-850	85.43	11.43	3.15
3D-NS-900	89.83	7.11	3.07
3D-NS-950	88.58	5.57	5.75

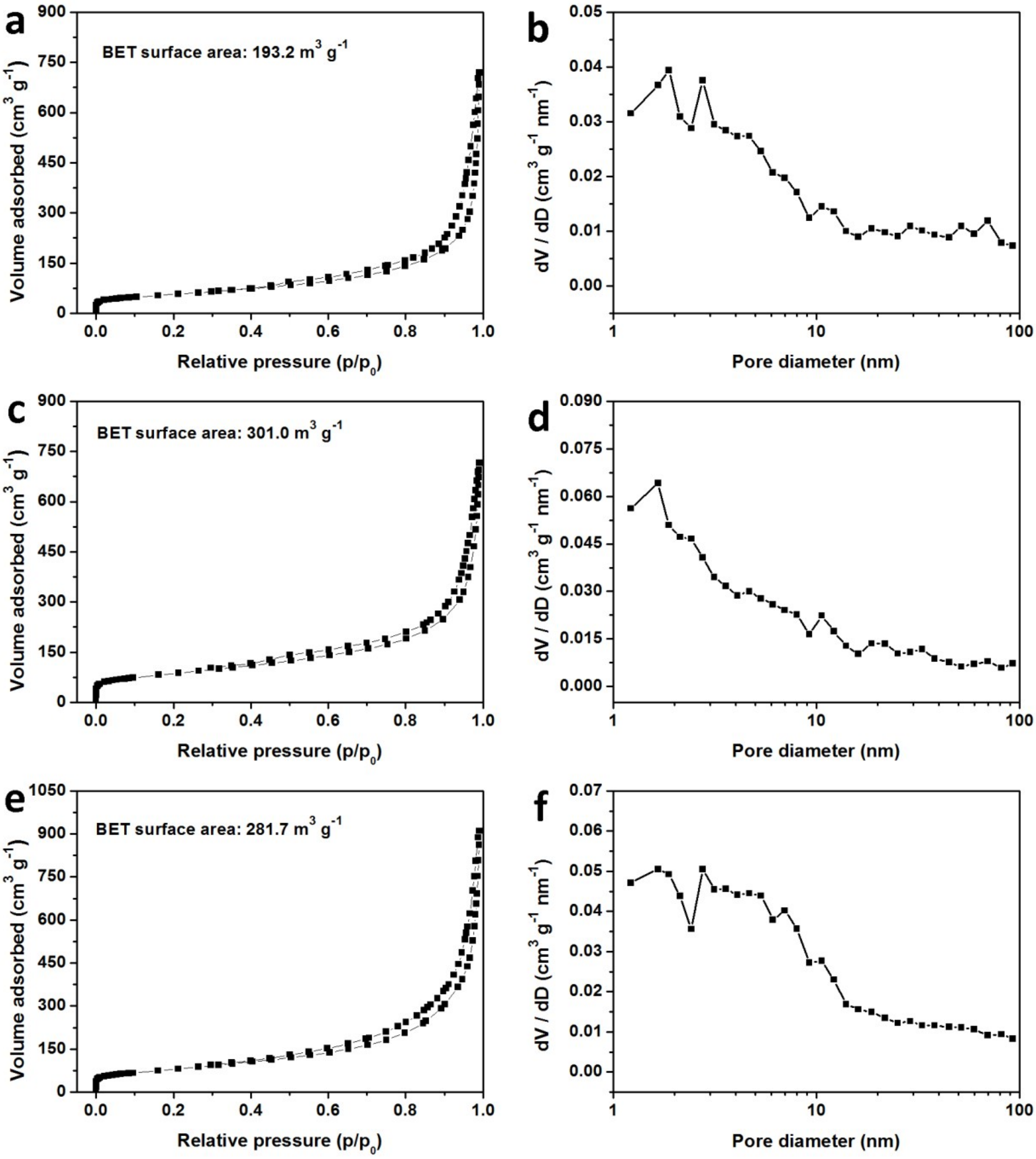

Fig. S10 Nitrogen adsorption/desorption isotherms and pore size distribution of (a) (b) 3D-NS-800 , (c) (d) 3D-NS-850 and (e) (f) 3D-NS-950.

Table S2 Pore characteristics of 3D-NSs.

samples	BET surface area ($m^2\ g^{-1}$)	total pore volume ($cm^3\ g^{-1}$)	average pore width (nm)
3D-NS-800	193.2	1.07	22.13
3D-NS-850	301.0	1.09	14.43
3D-NS-900	431.4	1.17	10.87
3D-NS-950	281.7	1.37	19.51

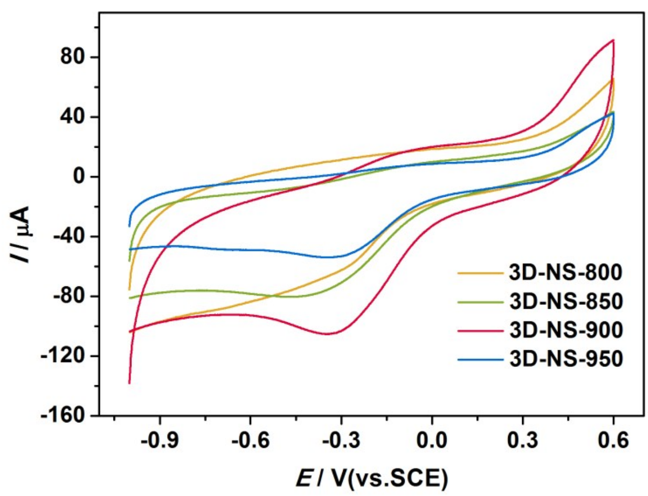

Fig. S11 CV curves of 3D-NSs modified electrodes in the presence of 5 mM H_2O_2.

Scan rate: 50 mV s^{-1}.

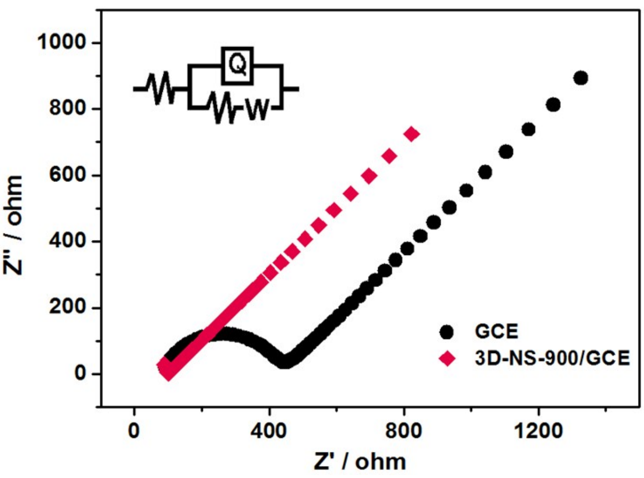

Fig. S12 EIS curves of GCE and 3D-NS-900/GCE in 0.1 M KCl solution with 10 mM $K_3[Fe(CN)]/K_4[Fe(CN)_6]$ (1:1). The frequency range of EIS was from 1×10^5 to 0.01 Hz with the amplitude of 5 mV. (insert) The equivalent circuit.

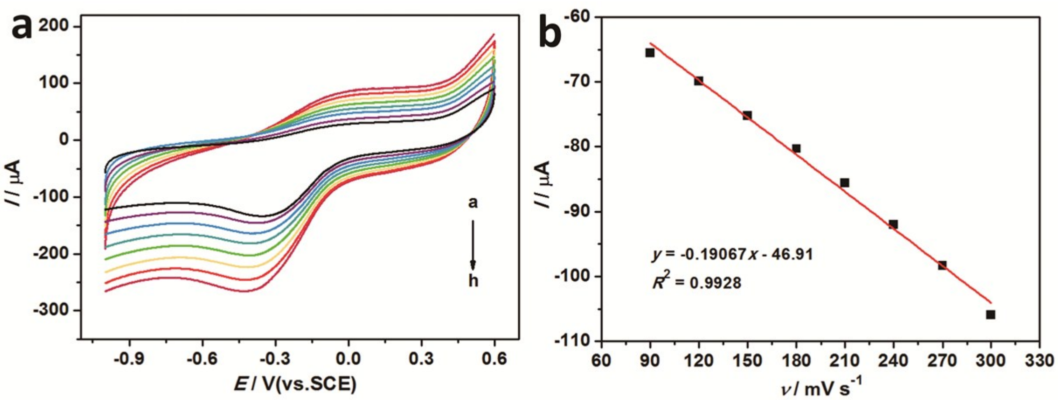

Fig. S13 (a) CV curves of 5 mM H_2O_2 at 3D-NS-900/GCE with different scan rates (90, 120, 150, 180, 210, 240, 270 and 300 mV s^{-1}) in 0.1 M PBS (pH 7.0). (b) The plot of cathodic peak current (I_{pc}) *vs*. Scan rate from 90 to 300 mV s^{-1}.

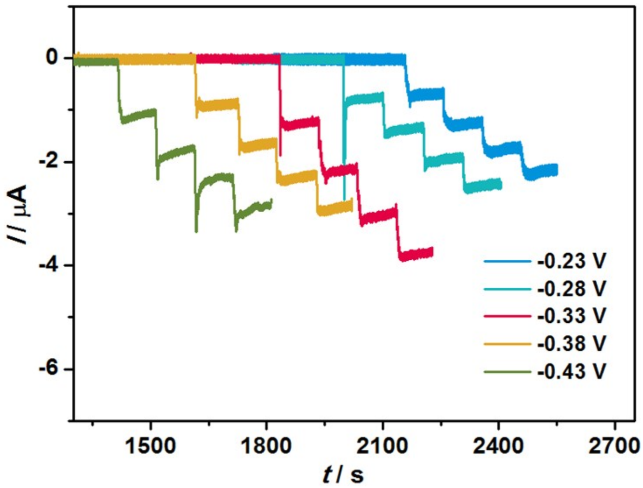

Fig. S14 The amperometric i-t curves of the 3D-NS-900/GCE with successive addition 100 μM H_2O_2 at different applied potentials.

The electrocatalytic behavior toward H_2O_2 at 3D-NS-900/GCE could be influenced by the detection potential in current-time (i-t) analytical technique. Therefore, the investigation of detection potential on i-t response was displayed in Fig. S14. Obviously, the maximum current response was obtained at −0.33 V in contrast to the others applied potentials. Hence, −0.33 V was chosen as the most favorable applied potential in the following study.

Table S3 Comparison of different modified electrodes for H_2O_2 determination.

Electrode	Linear range (μM)	Detection limit (μM)	References
ONPCNRs/SWCNT[a]/GCE	1-500	0.51	1
3D-N-Co-CNT@NG[b]/GCE	2-7449	2	2
HRP/peptides/Au[c]	0.1–100	0.03	3
Cu_2O/N-graphene/Nafion/GCE	5-3570	0.8	4
Co_3O_4-NWs/CF[d]/GCE	10-1400	1.4	5
AuPd@GR[e] 3:15/ITO	5-11500	1	6
Graphene-AuNPs/GCE	20-280	6	7
3D-NS-900/GCE	0.5–14000	0.18	This work

[a]ONPCNRs/SWCNT: oxygen-doped, nitrogen-rich carbon nanoribbons polymer and single-walled carbon nanotubes

[b]3D-N-Co-CNT@NG: 3D nanocomposite of nitrogen doped Co-CNTs over graphene sheets

[c]HRP/peptides/Au: horseradish peroxidase/ peptides/gold electrode

[d]Co_3O_4-NWs/CF: Co_3O_4 nanowires/carbon foam

[e]AuPd@GR: porous gold-palladium nanoalloy network-supported graphene

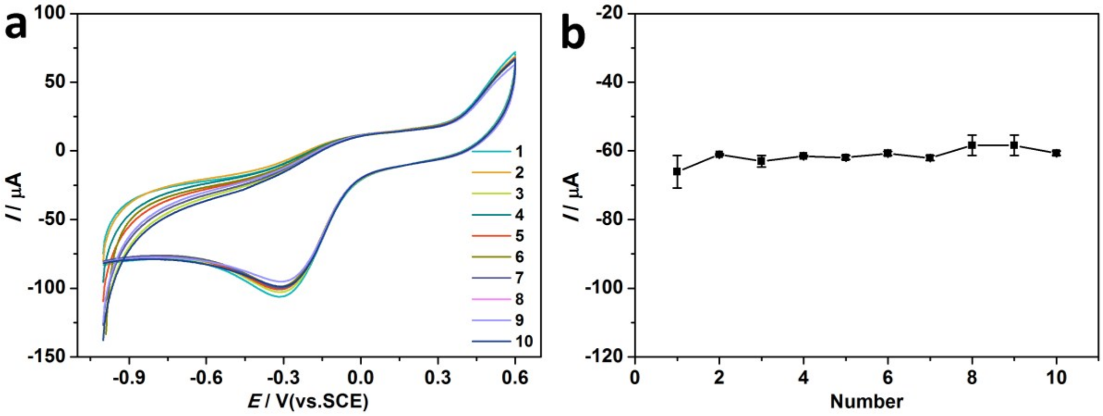

Fig. S15 (a) CV curves of 6 mM H_2O_2 with ten successive measurements at the same 3D-NS-900/GCE in 0.1 M PBS (pH 7.0). (b) The plot of cathodic peak current (I_{pc}) *vs*. the number of measurements. Scan rate: 50 mV s^{-1}.

Table S4. The comparison of different 3D-N doped carbon materials.

Materials	Number of measurements	RSD (%)	References
ONPCNRs/SWCNT[a]	5	5.40	[1]
3D N-Co-CNT@NG[b]	--	~4.20	[2]
3D-NGA[c]	10	6.30	[8]
3D NCNT[d]	6	3.90	[9]
3DNGE[e]	6	3.30	[10]
3D-NS[f]	10	3.73	This work

[a]ONPCNRs/SWCNT: oxygen-doped, nitrogen-rich carbon nanoribbons polymer and single-walled carbon nanotubes

[b]3D N-Co-CNT@NG: 3D nanocomposite of nitrogen doped Co-CNTs over graphene sheets

[c]3D-NGA: 3D nitrogen-doped graphene aerogel

[d]3D NCNT: 3D nitrogen-doped carbon nanotube

[e]3DNGE: 3D porous nitrogen-doped graphene modified Au electrode

[f]3D-NS: 3D N-doped porous carbon nanosheets

Table S5 Determination of H_2O_2 in Real Samples

Sample	Added(μM)	Found[a] (μM)	RSD (%)	Recovery (%)
Serum 1	50.00	51.91	1.05	103.80
Serum 2	170.00	164.71	0.65	96.90

[a] Average of five determinations.

References

1. Z.-X. Wang, J.-Y. Wang, X.-H. Yu, F.-Y. Kong, W.-J. Wang, W.-X. Lv, L. Ge and W. Wang, *Sensors and Actuators B: Chemical*, 2017, **246**, 726-733.
2. J. Balamurugan, T. D. Thanh, G. Karthikeyan, N. H. Kim and J. H. Lee, *Biosensors and Bioelectronics*, 2017, **89**, 970-977.
3. J. Zhao, Y. Yan, L. Zhu, X. Li and G. Li, *Biosensors and Bioelectronics*, 2013, **41**, 815-819.
4. B.-B. Jiang, X.-W. Wei, F.-H. Wu, K.-L. Wu, L. Chen, G.-Z. Yuan, C. Dong and Y. Ye, *Microchimica Acta*, 2014, **181**, 1463-1470.
5. M. Liu, S. He and W. Chen, *Nanoscale*, 2014, **6**, 11769-11776.
6. T. D. Thanh, J. Balamurugan, S. H. Lee, N. H. Kim and J. H. Lee, *Biosensors and Bioelectronics*, 2016, **85**, 669-678.
7. J. Hu, F. Li, K. Wang, D. Han, Q. Zhang, J. Yuan and L. Niu, *Talanta*, 2012, **93**, 345-349.
8. Z.-X. Cai, X.-H. Song, Y.-Y. Chen, Y.-R. Wang and X. Chen, *Sensors and Actuators B: Chemical*, 2016, **222**, 567-573.
9. M. Zhang, Z. Huang, G. Zhou, L. Zhu, Y. Feng, T. Lin, H. Hou and Q. Guo, *Analytical Methods*, 2015, **7**, 8439-8444.
10. Q. Yamin, B. Jie, D. Xiaoteng and Z. Hui‐Min, *Electroanalysis*, 2017, **29**, 2083-2089.